

Reconstruction of the Exenterated Orbit with an Island Pericranial Flap: A New Surgical Approach

Sophia Kuehnel*
 András Grimm, MD†
 Christopher Bohr, MD‡
 Werner Hosemann, MD§
 Rainer Weber, MD¶
 Tobias Ettl, MD||
 Thomas Kuehnel, MD‡

Background: Reconstruction of the bony socket after orbital exenteration is a matter of much debate. Prompt defect closure with a microvascular flap is desirable but involves a major surgical procedure and hence, places considerable burden on the patient. The new surgical technique presented here permits a technically simpler wound closure with fewer complications after orbital exenteration.

Methods: Between May 2014 and June 2022 in the ENT department of Regensburg University, nine patients underwent exenteration and reconstruction with a pericranial flap. The flap was raised via a broken line incision in the forehead or endoscopically, incised in a roughly croissant-like shape, then introduced into the orbit through a tunnel in the eyebrow. A retrospective analysis of the patients and considerations about determining the size, shape, and vascular supply of the flap are presented.

Results: Flap healing was uncomplicated in all cases. Only 6 weeks after surgery, the flap was stable, making it possible to start adjuvant therapy and prosthetic rehabilitation swiftly. The flap is adapted to the near cone-shape of the orbit. The mean (\pm standard deviation) surface area of the measured orbits is (39.58 ± 3.32) cm². The territory of the angular artery provides the periosteal flap arterial blood supply. Venous drainage is via venous networks surrounding the artery.

Conclusions: Use of the pericranial flap makes it possible to close the orbital cavity promptly with minimal donor site defect and a short operating time, thereby minimizing the surgical risk and speeding up physical and psychological recovery. (*Plast Reconstr Surg Glob Open* 2023; 11:e5082; doi: 10.1097/GOX.0000000000005082; Published online 12 July 2023.)

INTRODUCTION AND OBJECTIVE

Orbital exenteration classically entails removal of the entire orbital contents, including periosteum and eyelids (type I defect).¹ The primary indication is tumors, less commonly trauma or vascular malformation.² The

procedure leaves behind the exposed bone of the orbital cavity.³ The best possible postexenteration treatment is required to make the disfigurement caused by the surgery bearable for the patient. The aim is demarcation from surrounding tissues and swift reepithelialization of the defect, thus providing the foundation for adjuvant radiotherapy that is often required and for prosthetic rehabilitation. Secondary wound healing takes a long time.⁴ To shorten this time, various methods for covering the bone with soft tissue are available. Possible options to consider are split-skin graft, which is the simplest method; various local and regional flaps^{5,6}; or coverage with a microvascular flap, which is the most complex.^{7,8} Selection should be based on the patient's needs. We present here a surgical approach that is technically straightforward, promises rapid wound healing, and provides a good, flat recipient bed for an ocular prosthesis. The technical aspects, advantages, and disadvantages compared with other techniques and a retrospective analysis of nine patients are discussed.

From the *Department of Ophthalmology, University Hospital Wuerzburg, Wuerzburg, Germany; †Anatomical Institute, Semmelweis University, Budapest, Hungary; ‡Department of Otorhinolaryngology, University Hospital Regensburg, Regensburg, Germany; §ENT Department, Helios Hansekllinikum Stralsund, Stralsund, Germany; ¶ENT Clinic Karlsruhe, Karlsruhe, Germany; and ||Department of Maxillofacial Surgery, University Hospital Regensburg, Regensburg, Germany.

Received for publication February 6, 2023; accepted April 28, 2023.

Copyright © 2023 The Authors. Published by Wolters Kluwer Health, Inc. on behalf of The American Society of Plastic Surgeons. This is an open-access article distributed under the terms of the [Creative Commons Attribution-Non Commercial-No Derivatives License 4.0 \(CCBY-NC-ND\)](https://creativecommons.org/licenses/by-nc-nd/4.0/), where it is permissible to download and share the work provided it is properly cited. The work cannot be changed in any way or used commercially without permission from the journal.

DOI: 10.1097/GOX.0000000000005082

Disclosure statements are at the end of this article, following the correspondence information.

METHODS

Patients

We present nine patients who underwent orbital exenteration for a type I defect (with or without lid involvement) and socket reconstruction with pericranial flap surgery between May 2014 and June 2022 at the University of Regensburg. A retrospective analysis of the patient records was done, focusing on details of age, gender, diagnosis, orbital side involved, defect dimensions, type of reconstruction, adjuvant therapy, complications, and prosthetic rehabilitation (Table 1). Written consent for this surgical procedure and, if applicable, for publication of the enclosed image material was obtained from all patients.

Surgical Procedure

Exenteration and reconstruction of the orbit is performed in a single surgical session. If the eyelids can be preserved, their epidermis (without lashes) is later used in lining the orbital cavity. During exenteration the path of the angular artery must be observed, and the vessel avoided because it will later supply the flap. The main vessel supplying the medial pericranial area is the supra-trochlear artery though. Obviously, this vessel cannot be preserved as the ophthalmic artery is severed (Fig. 1).

To dissect the vascular pedicle, an artery above the eyebrow is located in the region medial to the vertical extension of the medial canthus⁹ and, once the flow rate has been checked by duplex ultrasound, the narrow flap pedicle is dissected in the cranial direction. It is important to protect the first branch of the trigeminal nerve and avoid the temporal fossa when the flap is being exposed.

Takeaways

Question: How to cover the bare bone of an exenterated orbit with a straight forward, safe and durable flap in a one stage procedure with low morbidity.

Findings: The study illustrates the surgical approach to cover the bony orbit after orbital exenteration using a newly designed pericranial flap with further investigations concerning the flap’s vascular supply and outline.

Meaning: A method for rapid, safe, and cosmetically favorable reconstruction of the exenterated orbit with a pedicled pericranial flap.

From about 1.5 cm above the vascular bundle, a near to 10-cm-long skin incision is made using the broken line technique. The scalp, consisting of cutis, subcutis and galea, forms a unit and can be readily undermined so that the layer consisting of periosteum, including subgaleal connective tissue, can be exposed.¹⁰ To simplify incision of the flap, methylene blue can be used beforehand to mark out points on the forehead. An endoscopic method for raising the flap is appropriate for younger patients as a way of avoiding visible scarring on foreheads, which are still unlined. For this purpose, a transverse skin incision is made in the hairline. After the periosteal layer has been mobilized, the flap is incised and, as for open reconstruction, is moved into the orbit through a previously created tunnel in the eyebrow. Fixation involves a bridle suture to the sturdy connective tissue of the annulus of Zinn and Vicryl interrupted sutures to the periosteum of the orbital rim. Conically trimmed split skin grafts harvested from the medial face of the upper arm are sewn onto the periosteal

Table 1. Demographic Data of Patients

Pati	Age and Gender	Diagnosis	Orbit Involved (R/L)	Spread Beyond Orbit and Lid Involvement	Type of Reconstruction	Adjuvant Therapy	Complications	Prosthesis
1	43/man	Plasmocytoma	R	No	Periosteal flap, split skin graft	No	None	No
2	60/man	Squamous cell carcinoma	R	No	Periosteal flap, split skin graft	No	None	No
3	74/man	Basal cell carcinoma	L	Upper and lower lid, parts of root, and side of nose	Periosteal flap, split skin graft	No	None	Yes
4	81/man	Squamous cell carcinoma	R	Lower lid, rim around orbit	Periosteal flap, split skin graft	Postoperative systemic therapy	None	Yes
5	87/man	Squamous cell carcinoma	L	Lower lid, ethmoid, lacrimal ducts	Periosteal flap (endoscopic), split skin graft	No	Infection in area of titanium anchors	Yes
6	85/man	Squamous cell carcinoma	R	Lower lid	Periosteal flap, split skin graft	No	None	Yes
7	79/woman	Conjunctival melanoma	R	Upper and lower lid, lacrimal ducts	Periosteal flap, split skin graft	Postoperative radiotherapy	None	Yes
8	83/woman	Poorly differentiated, nonsmall cell carcinoma of uncertain entity	R	Upper lid, lacrimal ducts, erosion of cranial orbital roof	Periosteal flap, split skin graft	Postoperative systemic therapy	None	No
9	74/woman	Squamous cell carcinoma	L	Lower lid, infraorbital rim	Periosteal flap, split skin graft	No	None	yes

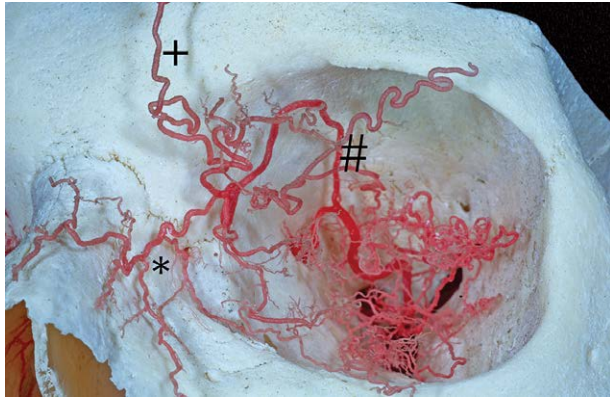


Fig. 1. Corrosion cast specimen of arteries around the left orbit. Arterial supply of a pericranial flap after orbital exenteration is provided via the angular artery (*) with its peripheral forehead-branches and/or anastomoses with the peripheral supratrochlear artery (#). Resulting feeding vessel of the pericranial flap (+).

layer for faster epithelialization. The orbit is packed with a gentle pressure dressing, which is left in place for 10 days. If required, osseointegrated implants for fitting a magnet-retained orbital prosthesis are placed according to the two-stage method described by Nerad.¹¹ If a patient is undergoing radiotherapy, we do not start the placement of implants until after the adjuvant therapy is completed.

Basic Research on Flap Size and Design

Initially, the basic shape (geometry) of flaps to cover the entire orbital wall was determined in an anatomical model: a silicone cast of the orbital cavity was created on the anatomical preparation, the outer surface being stained then rolled onto paper. This enabled the three-dimensional orbital body to be depicted as a flat two-dimensional outline. The rectangular flap design that has hitherto been used in orbital reconstruction served as an additional guide.⁵⁻¹³ These contours were cut out of tissue-like material and tested on a cranial model. The flap design was optimized for minimum cutting loss.

Corrosion cast specimens, which had been prepared at the Anatomical Institute, Semmelweis University, Budapest, were used to depict the preoperative vascular anatomy in the forehead area.

In addition, the surface area of the bony orbital cavity was calculated from CT data sets to determine the minimum size of flap required. Very high resolution (0.65 mm sections) CT data sets from 11 White body donors were available, the dimensions having been measured for both orbits. We defined the orbit as roughly conical. In the data set, this conical shape can be divided into individual truncated cones, of which the lateral surface areas can be calculated layer-by-layer by means of measurements of orbit circumference in coronal section. The total surface area of the orbital cavity is obtained by adding together the lateral surface areas of the individual truncated cones (Fig. 2).

The apex of the cone forms the lowest-lying point of the orbit and, in our measurements, is defined by the anterior edge of the intersection of the extraocular

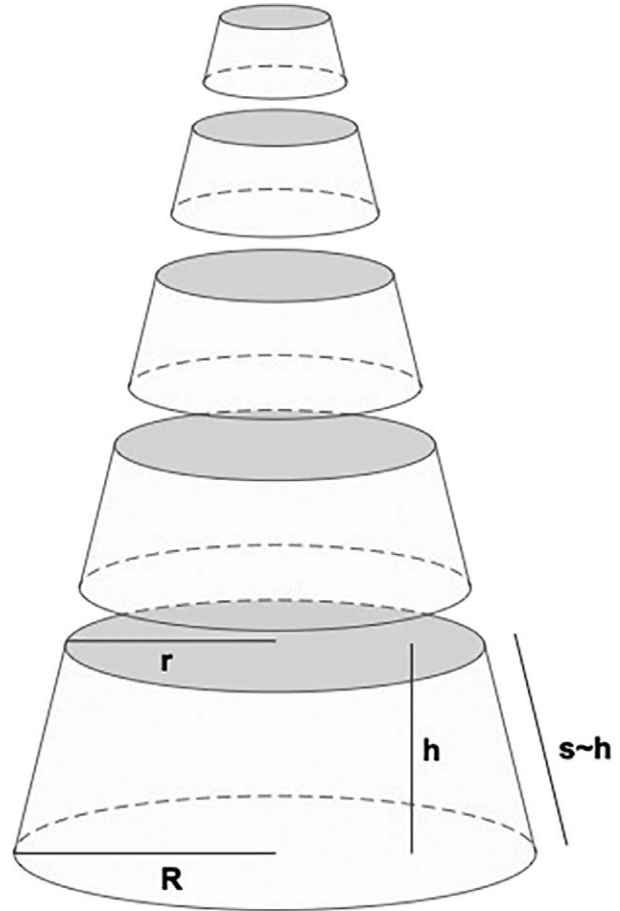


Fig. 2. The orbit depicted as a cone and divided into truncated cones, of which the lateral surface areas can be calculated with the formula $L_c = \pi \times s \times (R + r)$.

muscle tracts in the axial CT section. The base of the cone equates to the width of the orbit, which is defined by the distance between the medial and lateral margins. The measuring point on the medial margin is the intersection between the extension of the anterior lacrimal crest and the frontomaxillary suture. The measuring point on the lateral margin lies in the same plane as the medial margin and it is marked by the intersection with the lateral orbital rim. The formula for the lateral surface area of the truncated cone is $L_c = \pi \times s \times (R + r)$, where the slant height “s” equates to the height of the truncated cone [R, r: radius of the circular base and deck area of the truncated cone]. Using the Novaplan 2.6.17 CE program, coronal images of the orbit were depicted in 2-mm slices, and the orbital circumference was measured using the Lasso tool in Photoshop CC 2018. The radius is determined from the circumference: $r = C \div (2 \times \pi)$.

The superior and inferior margins of the orbit are more anteriorly located than the cone base defined by us at the level of the line connecting medial to lateral margin. To allow for the area that is lacking, a cylinder lateral surface area $L_{cy} = 2 \pi \times r \times h$ was added to the lateral surface area of the cone, with its height equating to the distance between the line from medial to lateral margin

and the line connecting superior to inferior margin [r: radius]. The orbital width at the height of the plane of the orbital entrance was used as the radius. In all cases, calculations were done on values rounded to whole millimeters.

RESULTS

Patients

The new surgical approach has so far been used in nine patients, aged between 43 and 87 years. All of them had an oncological tumor diagnosis as an underlying disease (Table 1). The indication for orbital exenteration was established by means of computed tomography or magnetic resonance imaging, histologic identification of the tumor entity, and investigations regarding operability. Patients were informed about alternative methods such as radiotherapy and chemotherapy. The prerequisite was that the defect should be largely confined to the orbital contents and no bony structures or sizeable skin areas outside the orbit should be involved. The decision-making process was not influenced by involvement of the eyelids, the use of adjuvant radiotherapy and/or systemic therapy, or the wish for prosthetic rehabilitation.

The operation was successfully carried out in all patients. One patient developed an intraoperative blood pressure crisis with a fall in saturation levels so that the operation was stopped after exenteration and reconstruction was continued in a second session. For all the other patients, exenteration and reconstruction were performed in a single session. Postoperative progress was normal. The flaps healed without complication and without requiring

further surgical measures. There were no instances of venous congestion, necrosis, or flap shrinkage. None of the patients received neoadjuvant therapy. The postoperative adjuvant therapy did not impede the healing process. The dressing was first changed and wound healing was checked after about 10 days, and a second appointment was arranged for six weeks later. No further visits to the doctor were necessary because patients were able to carry out the minimal care of the cavity themselves. Six weeks after surgery, the flaps were already stable enough for the commencement of radiotherapy and/or systemic therapy if required. Once the adjuvant therapy was completed, titanium anchors were implanted in a second operation for patients requesting prosthetic rehabilitation, and the abutments were placed under local anesthesia three to four months later. Prosthesis fitting was possible another 4 weeks later. After implantation of the titanium anchors, one patient developed an orbital infection, which resulted in revision involving split-skin coverage. Fitting of osseointegrated implants was problem-free for all the other patients (Fig. 3).

Flap Size and Design

A rectangular flap shape results in areas of excess tissue in the region of the medial and lateral canthus, which must be adapted and sutured. Incising a more or less crescent-shaped flap and rotating it into the orbit produces a single incised edge and less excess material. Arterial supply to the periosteal flap comes from the angular artery (Figs. 4, 5).

This anastomoses with the supratrochlear artery in the area of the supraorbital rim, or it sends out direct

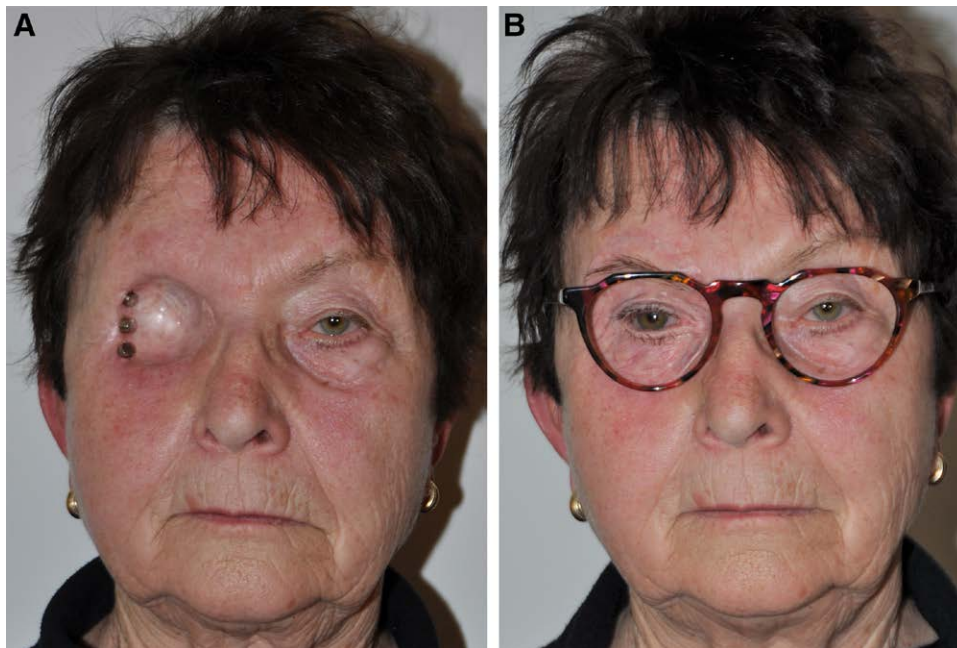


Fig. 3. An 82-year-old female patient, 15 months after right-sided orbital exenteration with immediate reconstruction by means of a pericranial flap. Specific implants (A) provide fitting and fixation of an epithetic device (B).

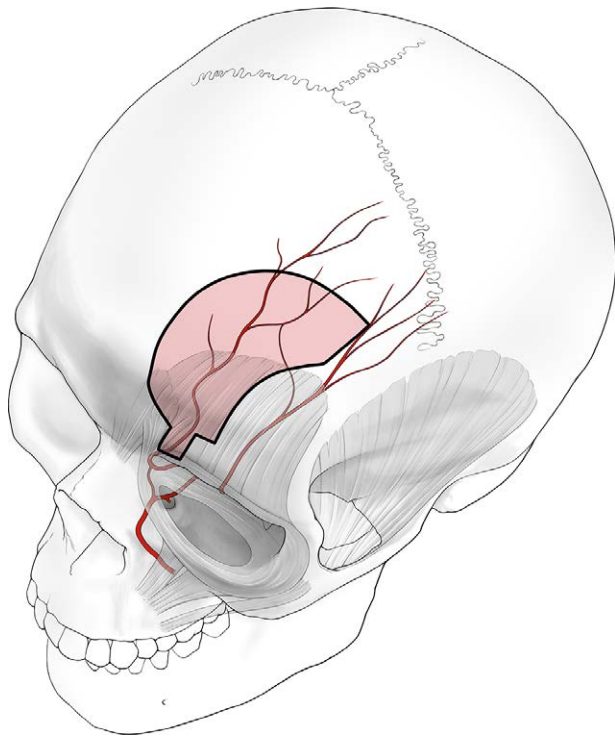


Fig. 4. Schematic outline of a left-sided pericranial flap before harvesting.

branches to the forehead.^{14,15} The corrosion cast specimen reveals the exposed position of the anastomosis to the supratrochlear artery. The flap pedicle is always narrowly dissected with a width of around half a centimeter. This enables the flap to be transposed into the orbit under the eyebrow tunnel, while the incision path becomes virtually invisible. (Fig. 6).

The measurements used to calculate the surface area of the orbit were rounded to whole millimeters in all cases. The correlations were calculated using the Spearman correlation test, and the level of significance was set at 0.05. The mean (\pm standard deviation) surface area of the measured orbits was $39.58 \pm 3.32 \text{ cm}^2$. Large interindividual differences were noted, with values of $33.46\text{--}46.38 \text{ cm}^2$. The intraindividual difference between right and left orbit was not significant ($P = 0.85$). Three measurements were repeated, with a measurement error of up to 3.1% being recorded. There is a significant positive correlation (correlation = 0.87, $P = 1.32 \times 10^{-7}$) between orbit surface area and orbit depth.

DISCUSSION

Pericranial flaps are a familiar feature of craniofacial surgery.^{12–16} The use of a pericranial rotation flap pedicled at the medial forehead for lining the cavity after orbital exenteration is a novel approach, though.^{17–19} The delicate periosteal layer is particularly suitable for reconstruction in the facial area. An epidermal layer is harder to adjust to the complex concave cavity and therefore has not been considered.

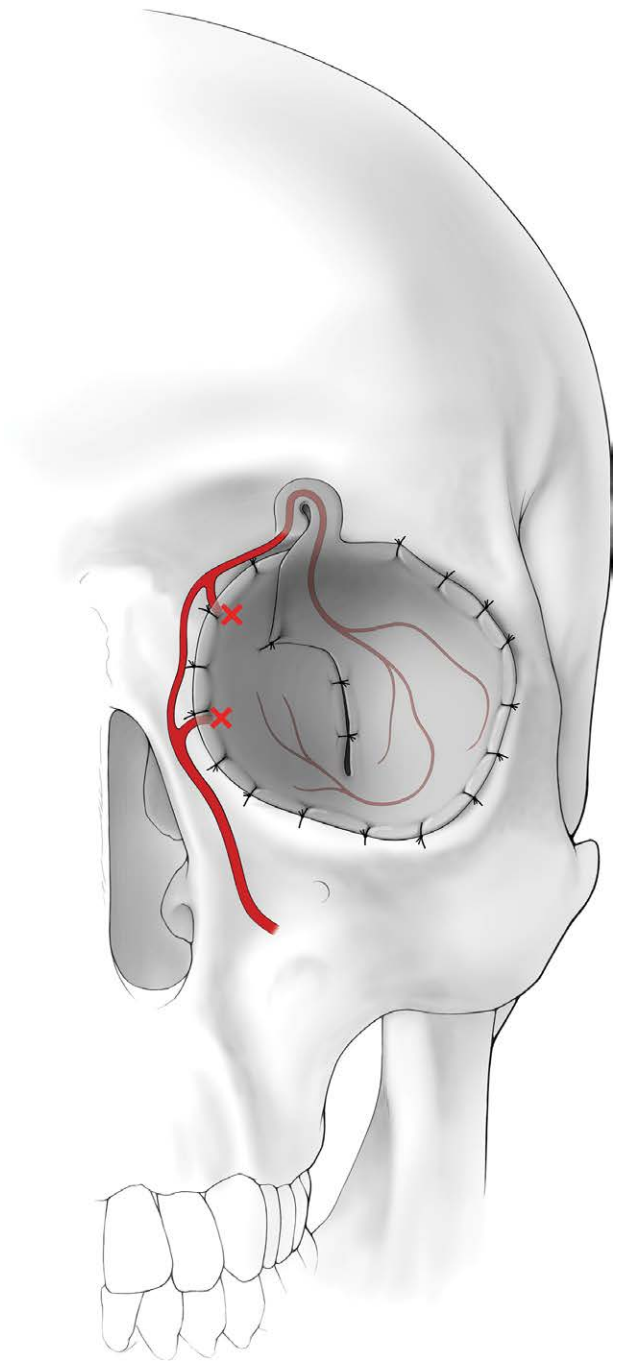


Fig. 5. Schematic illustration of a left-sided pericranial flap secured in the final position highlighting the looping arterial supply.

The periosteal tissue in combination with a split skin graft, however, is a good match for the surrounding tissue in terms of color and structure, and it provides a thin prosthetic bed.¹² Recurrences can be detected more quickly through the thin skin covering than with voluminous flaps. The fact that the periosteal layer can be mobilized over a large area means that the whole orbit can be lined and demarcation from surrounding structures can be achieved without difficulty. Another

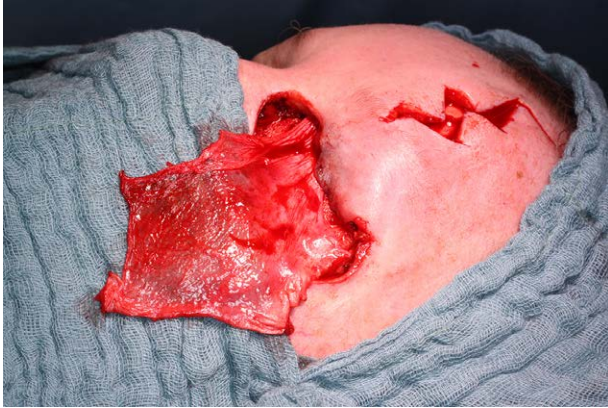


Fig. 6. Orbital reconstruction following left-sided exenteration. Harvest of a pericranial flap via a prefrontal "broken line" incision.

advantage of the approach via a broken-line incision or endoscopic mobilization through a skin incision inside the hairline is minimal donor site defect and barely perceptible scar formation on the forehead. The vascular situation in the forehead area must be borne in mind when the flap pedicle is being dissected. During exenteration, the supratrochlear artery is severed as it passes through the orbit, but the blood flow from the territory of the angular artery is sufficient to perfuse the flap satisfactorily.²⁰ After exenteration, a vessel above the brow is located approximately in the extension of the medial canthus and dissected in the cranial direction. This may be a direct branch of the angular artery or the supratrochlear artery fed via anastomosis. In many cases, deep branches to the periosteum are only given off after as much as 1.5 cm. Therefore, the flap pedicle should not be degenerated.^{21,22} Furthermore, venous drainage via the flap pedicle must be guaranteed to prevent congestion. It is reported that a network of fine veins wind around the supratrochlear artery and ultimately flow into the periorbital veins.²³ This makes it possible to dissect a narrow flap pedicle. Integration of larger-lumen veins into the pedicle may play a greater role in the case of more voluminous cutaneous grafts.¹⁴⁻²³

There is no consensus about the height at which the periosteal vessels end, and hence, avascularity of the flap is imminent.¹⁵⁻²⁴ Necrosis has never been observed after orbital reconstruction with periosteal flap surgery when the dissection extended beyond the border of the hairline. However, this may occur, as in any flap design, and its frequency could only be judged by a far larger number, as in our study.

The group presented here reflects most patients for whom orbital exenteration is indicated; they are predominantly patients of advanced age with comorbidities. The approach presented here allows for surgery to be performed swiftly in a single session and with few complications. The aesthetic outcome is in no way inferior to that of other reconstruction techniques. If prosthetic rehabilitation is desired, a magnet-retained orbital prosthesis is recommended because this most closely resembles the natural appearance and delivers the most

appealing results both visually and functionally.²⁵ Owing to the good vascularization of the periosteum, it seems that the required implantation of titanium anchors can also be done in one session, immediately after exenteration, thereby sparing the patient a further surgical procedure.¹² The approaches to orbital reconstruction hitherto described in the literature all entail some compromise. The different approaches need to be considered afresh for each patient, depending on the size of defect, planned adjuvant therapy, and the desire for prosthetic rehabilitation.²⁶ With open granulation or split skin grafts sewn on, the approach is minimally invasive, but the wound healing process will take weeks to months. If the wound healing process needs to be sped up, reconstruction with a temporalis muscle flap is a gold standard.²⁷⁻³²

Drawbacks are that the orbital rim has to be fenestrated for rotating the flap into the cavity³³ and, after displacement of the muscle, visible loss of volume in the temporal region often ensues.¹ Masticatory discomfort is a possibility. Another potential complication is paralysis of the frontal branch of the facial nerve.³² Owing to the limited area of the temporalis flap, it does not reliably reach the medial portions of the orbit.¹ Dehiscence frequently occurs in the medial wall of the orbit formed by the ethmoid, so that discharge from the nose and its accessory sinuses escapes into the orbital wound during the wound healing phase and can impair wound healing. If defect dimensions spread to bony structures and/or large areas of skin, different reconstruction techniques will be employed. Microvascular myocutaneous or fasciocutaneous flaps^{7,8} can be configured large enough and are notable for their stability. However, they are not used as a standard because the microvascular surgery required for raising such flaps is challenging and time-consuming⁵ and because they are clearly distinguishable from the facial tissue in color and texture. These flaps often require secondary thinning before prosthetic fitting because of their volume.⁷ The new approach presented here can be used whenever a case is operable and the type I defect dimensions are not exceeded. The choice can be made irrespective of adjuvant therapy, prosthetic rehabilitation, or age, which greatly simplifies the decision-making process. However, surgery should be executed before irradiation if possible, as it seems to be the functional status of the bed tissue that is crucial for healing of the flap. Postoperative irradiation usually does not jeopardize a vital flap.

To standardize this approach for use in type I defects, we wanted to establish the required flap size and shape. Calculations of the surface area of the orbital cavity are hardly reported in the literature. However, Felding et al³⁴ report of the surface area in 26 orbits that was measured between orbital apex and the plane of the orbital entrance (height: line connecting medial to lateral margin), resulting in measurements between 28.21 and 38.44 cm², which coincide closely with our measurements of the orbital surface from apex to the plane of the orbital entrance (26.60 and 40.59 cm²). The large interindividual differences in orbit size and shape are also reflected in the data from the literature.³⁵ As the graft needs to

line the surface up to the orbital rim and the superior and inferior margins are more anteriorly placed than the plane of the orbital entrance, another cone segment was added in our measurements, taking as its height the distance between orbital entrance plane and the line connecting inferior to superior margin. Finally, this produces total surface areas between 33.46 and 46.38 cm². As there is a significant correlation between orbital surface area and orbital depth, the depth can be measured preoperatively on a CT image and can provide an indication of the approximate dimensions of the orbital cavity to be covered. In textbooks the average depth is given as 39–50 mm^{35,36}; in our specimen, the average depth is 42 mm. If the orbit is seemingly bigger or smaller, the flap should be tailored to the approximate difference. A limitation of the study is that we did not consider tissue elasticity. With regard to the clinical relevance, the calculated flap design is a theoretical number. Flaps align to the area they should cover quite nicely even if they do not fit accurately when harvested.

Thomas Kuehnel, MD

Department of Otorhinolaryngology
University Hospital Regensburg
Franz-Josef-Strauss-Allee 11
D-93053 Regensburg
Germany
E-mail: thomas.kuehnel@ukr.de

DISCLOSURE

The authors have no financial interest to declare in relation to the content of this article.

PATIENT CONSENT

The patient provided written consent for the use of her image.

ACKNOWLEDGMENT

The protocol was approved by the institutional review board of the university of Regensburg (No. 21-2415-104).

REFERENCES

1. Kesting MR, Koerdt S, Rommel N, et al. Classification of orbital exenteration and reconstruction. *J Craniomaxillofac Surg.* 2017;45:467–473.
2. Keutel C, Hoffmann J, Besch D, et al. Orbitale exenteration. Therapiealgorithmus und rehabilitation [Orbital exenteration. Algorithm for therapy and rehabilitation]. *Ophthalmologe.* 2011;108:1023–1026.
3. Qassem A, Aljudaibi N, Wavreille O, et al. Orbital exenteration and periorbital skin cancers. *J Oral Maxillofac Surg.* 2014;72:811–816.
4. Putterman AM. Orbital exenteration with spontaneous granulation. *Arch Ophthalmol.* 1986;104:139–140.
5. Rodrigues ML, Kohler HF, Faria JC, et al. Reconstruction after extended orbital exenteration using a fronto-lateral flap. *Int J Oral Maxillofac Surg.* 2009;38:850–854.
6. Torroni A, Cervelli D, Gasparini G, et al. Anterior retrograde approach to the myofascial temporalis muscle for orbital reconstruction: series of 9 consecutive cases. *Ann Plast Surg.* 2015;74:37–42.
7. Cherubino M, Berli J, Turri-Zanoni M, et al. Sandwich fascial anterolateral thigh flap in head and neck reconstruction: evolution or revolution? *Plast Reconstr Surg Glob Open.* 2017;5:e1197.
8. Purnell CA, Vaca EE, Ellis MF. Conical modification of forearm free flaps for single-stage reconstruction after total orbital exenteration. *J Craniofac Surg.* 2017;28:e767–e769.
9. Ugur MB, Savranlar A, Uzun L, et al. A reliable surface landmark for localizing supratrochlear artery: medial canthus. *Otolaryngol Head Neck Surg.* 2008;138:162–165.
10. Fu CH, Hao SP, Hsu YS. Use of a galeopericranial flap for the reconstruction of anterior cranial base defects. *Chang Gung Med J.* 2005;28:341–348.
11. Nerad JA, Carter KD, LaVelle WE, et al. The osseointegration technique for the rehabilitation of the exenterated orbit. *Arch Ophthalmol.* 1991;109:1032–1038.
12. Cameron M, Gilbert PM, Mulhern MG, et al. Synchronous reconstruction of the exenterated orbit with a pericranial flap, skin graft and osseointegrated implants. *Orbit.* 2005;24:153–158.
13. Tse DT, Goodwin WJ, Johnson T, et al. Use of galeal or pericranial flaps for reconstruction or orbital and eyelid defects. *Arch Ophthalmol.* 1997;115:932–937.
14. Kleintjes WG. Forehead anatomy: arterial variations and venous link of the midline forehead flap. *J Plast Reconstr Aesthet Surg.* 2007;60:593–606.
15. Reece EM, Schaverien M, Rohrich RJ. The paramedian forehead flap: a dynamic anatomical vascular study verifying safety and clinical implications. *Plast Reconstr Surg.* 2008;121:1956–1963.
16. Snyderman CH, Janecka IP, Sekhar LN, et al. Anterior cranial base reconstruction: role of galeal and pericranial flaps. *Laryngoscope.* 1990;100:607–614.
17. Battista RA, Giordano L, Giordano Resti A, et al. Combination of Mustarde cheek advancement flap and paramedian forehead flap as a reconstructive option in orbital exenteration. *Eur J Ophthalmol.* 2021;31:1463–1468.
18. Bilge AD, Yazici B, Efe AC. Reconstruction of orbital exenteration defect with cheek or combined cheek and forehead advancement flaps. *Ophthalmic Plast Reconstr Surg.* 2021;37:346–351.
19. Kovacevic P, Djordjevic-Jocic J, Radojkovic M. Lateral frontal galeal-cutaneous flap for reconstruction after orbital exenteration for advanced periorbital skin cancer. *Turk J Med Sci.* 2021;51:359–367.
20. McCarthy JG, Lorenc ZP, Cutting C, et al. The median forehead flap revisited: the blood supply. *Plast Reconstr Surg.* 1985;76:866–869.
21. Yoshioka N, Rhoton AL, Jr. Vascular anatomy of the anteriorly based pericranial flap. *Neurosurgery.* 2005;57:11–6; discussion 11.
22. Sertel S, Pasche P. Pericranial Flap for inner lining in nasal reconstruction. *Ann Plast Surg.* 2016;77:425–432.
23. Shimizu Y, Imanishi N, Nakajima T, et al. Venous architecture of the glabellar to the forehead region. *Clin Anat.* 2013;26:183–195.
24. Potparic Z, Fukuta K, Colen LB, et al. Galeo-pericranial flaps in the forehead: a study of blood supply and volumes. *Br J Plast Surg.* 1996;49:519–528.
25. Schoen PJ, Raghoebar GM, van Oort RP, et al. Treatment outcome of bone-anchored craniofacial prostheses after tumor surgery. *Cancer.* 2001;92:3045–3050.
26. Hanasono MM, Lee JC, Yang JS, et al. An algorithmic approach to reconstructive surgery and prosthetic rehabilitation after orbital exenteration. *Plast Reconstr Surg.* 2009;123:98–105.
27. Nassab RS, Thomas SS, Murray D. Orbital exenteration for advanced periorbital skin cancers: 20 years experience. *J Plast Reconstr Aesthet Surg.* 2007;60:1103–1109.
28. Mohr C, Esser J. Orbital exenteration: surgical and reconstructive strategies. *Graefes Arch Clin Exp Ophthalmol.* 1997;235:288–295.

29. Rahman I, Cook AE, Leatherbarrow B. Orbital exenteration: a 13 year Manchester experience. *Br J Ophthalmol.* 2005;89:1335–1340.
30. Cinar C, Arslan H, Bingöl UA, et al. The new anatomical classification system for orbital exenteration defect. *J Craniofac Surg.* 2017;28:1687–1693.
31. Kuiper JJ, Zimmerman MB, Pagedar NA, et al. Perception of patient appearance following various methods of reconstruction after orbital exenteration. *Orbit.* 2016;35:187–192.
32. Uyar Y, Kumral TL, Yildirim G, et al. Reconstruction of the orbit with a temporalis muscle flap after orbital exenteration. *Clin Exp Otorhinolaryngol.* 2015;8:52–56.
33. Menon NG, Giroto JA, Goldberg NH, et al. Orbital reconstruction after exenteration: use of a transorbital temporal muscle flap. *Ann Plast Surg.* 2003;50:38–42.
34. Felding UA, Bloch SL, Buchwald C. The dimensions of the orbital cavity based on high-resolution computed tomography of human cadavers. *J Craniofac Surg.* 2016;27:1090–1093.
35. Lanz T, Wachsmuth W. *Praktische Anatomie [Practical Anatomy]*. Berlin: Springer-Verlag; 2004.
36. Drake R, Vogl A, Mitchell A. *Gray's Anatomy for Students*. 2nd ed. Churchill Livingstone; 2009.